Electronic Supplementary Material (ESI) for Soft Matter.


# Determining the Elasto-adhesion Length by Void Collapse in Ultra-soft materials

Hongbo Fu[a] and Alfred J. Crosby[*a]

*a.Polymer Science and Engineering Department, University of Massachusetts, Amherst, MA 01003, USA. Email: acrosby@umass.edu*

## S1. Hydrogel preparation

We prepare polyacrylamide (PAM) hydrogels based on the solvent polymerization approach. The hydrogel preparation is conducted in a glove box with a nitrogen atmosphere to avoid oxygen contamination, except for the cured-in-air hydrogels mentioned in section 3.4 of the main text. PAM precursor solution with a weight concentration of 5% and the weight ratio of crosslinker to the monomer 1:100 is poured into a 20ml vial. The initiator APS (150μL,10wt% aqueous solution) and catalyst TEMED (15μL) is added to the solution to initiate polymerization, and the solution is stirred for 60 seconds. After removing the stir bar, the PTFE sheet is set in the solution. The PTFE sheet is hung on the cap before putting it in the vial, and thus the separator doesn't tilt during curing. The separator remains in the hydrogel until being used for the void collapse inspection method.

To prepare the PAM spherical probe, we transfer the precursor solution after adding APS and TEMED with a micropipette to a PTFE substrate. The liquid droplet forms a spherical cap due to the surface tension, and this shape remains until the liquid is fully cured. The spherical probe will have a radius curvature of ~8mm and a thickness of ~2mm if the transferred volume is ~150μL. A representative image of spherical hydrogel is shown in Figure s1(d).

To prepare the PAM substrate, we pour the PAM precursor solution into a cylindrical plastic Petri dish with dimensions 35mm*9.5mm (diameter*height). The precursor

solutions will be cured in the Petri dish with PTFE covering during the polymerization reaction.

## S2. Young's moduli with indentation

### S2.1 Flat probe indentation for Young's moduli of PAM hydrogels

Young's moduli of hydrogel in vials and cylindrical hydrogel substrates are measured with the flat probe indentation test, as shown in Figure s1(a). The force and displacement are collected by Texture Analyzer (model name: TA-XT plus) from Stable Micro Systems. The flat steel probe has a diameter of 2mm. The Young's modulus is calculated with the following algorithm[1–3]:

$$E = \frac{3}{8Ca}\left(1 + 1.33\left(\frac{a}{h}\right) + 1.33\left(\frac{a}{h}\right)^3\right)^{-1}. \quad \text{(s1)}$$

Here we assume $\nu = 0.5$ for PAM hydrogels and $C = \frac{d\delta}{dP}$ is the compliance at the small strain regime (~0.1mm after contact, as shown in Figure s1(b)), a is the contact radius valued as 1mm, and h is the thickness of the hydrogel sample, which is approximately 35mm and 9mm for hydrogels in vials and in Petri dish, respectively.

### S2.2 Indentation test for spherical probe hydrogels

Young's moduli of spherical probes are measured by an indentation test. The spherical hydrogel is actuated to the glass slide substrate, during which we collect the contact radius, resistance force, and displacement (Figure s1(c)). A linear relationship is valid to fit Young's modulus[4]:

$$\frac{2}{3} f_C f_P \delta_H - f_\delta \delta_H + \delta' = \left(\frac{1-\nu^2}{E}\right)\frac{1}{2a} f_C P', \quad \text{(s2)}$$

where δ' and P' are the displacement and resistant force collected from the Texture Analyzer, respectively; $\delta_H = \frac{a^2}{R}$ is the Hertzian contact; R is the radius of curvature of spherically shaped hydrogels. $f_C$, $f_P$, and $f_\delta$ are the finite thickness modification for Hertzian contact as a function of contact radius a and hydrogel thickness h[1,5]. The force, displacement, and time are collected on the Texture Analyzer (model name: TA-XT plus) from Stable Micro Systems. The video of contact is captured by a USB camera (model name: EO-50231M) from Edmund Optics. The contact radius is captured from the video. In this test, the interfacial energy between the PAM hydrogel probe and the glass substrate is strong and generates obvious hysteresis in the force-displacement curve. Young's modulus of the hydrogel probe is analyzed by the algorithm shown above, which is derived based on the Hertzian contact mechanics in the presence of adhesion energy[3–5]. The system compliance is expressed as

$$C = \frac{\delta - \delta'}{P - P'}. \quad \text{(s3)}$$

Here δ, P are the displacement and force in the presence of adhesion energy, δ' P' are the displacement and force in the absence of adhesion energy, and C is the compliance of the system. The displacement in the absence of adhesion follows the expression:

$$\delta' = \delta_H * f_\delta. \quad \text{(s4)}$$

Here $\delta_H = \frac{a^2}{R}$, which is the displacement in the Hertzian contact and $f_\delta = 0.4 + 0.6 * e^{-\frac{1.8a}{h}}$, which is the correction function of the displacement for the finite thickness. R is the radius of curvature of the spherical probe. The force in the absence of adhesion follows the expression:

$$P' = P_H * f_P \tag{s5}$$

Here $P_H = \frac{16Ea^3}{9\ R}$ is the contact force in the Hertzian contact and $f_P = 1 + 0.15\left(\frac{a}{h}\right)^3$ is the correction function for the finite thickness. Also, the system compliance still follows Equation s3, which is re-written as:

$$C_H f_H = \frac{\delta - \delta_H * f_\delta}{P - P_H * f_P}. \tag{s6}$$

Here $C_H = \frac{3}{8Ea}$ and $P_H = \frac{16Ea^3}{9\ R}$ include E in the expressions. Equation s6 can be rearranged as:

$$\delta + \left(\frac{2}{3} f_C f_P - f_\delta\right)\delta_H = \frac{1\ 3}{E8a} f_C P. \tag{s7}$$

In the expression, δ, P and a are extracted from experimental data, $f_C$, $f_P$, $f_\delta$ and $\delta_H$ are functions of a. The linear relationship is determined to fit Young's modulus. Our experimental data shows that the linear relationship is valid in both the indentation region and the retraction region (Figure s1(d)).

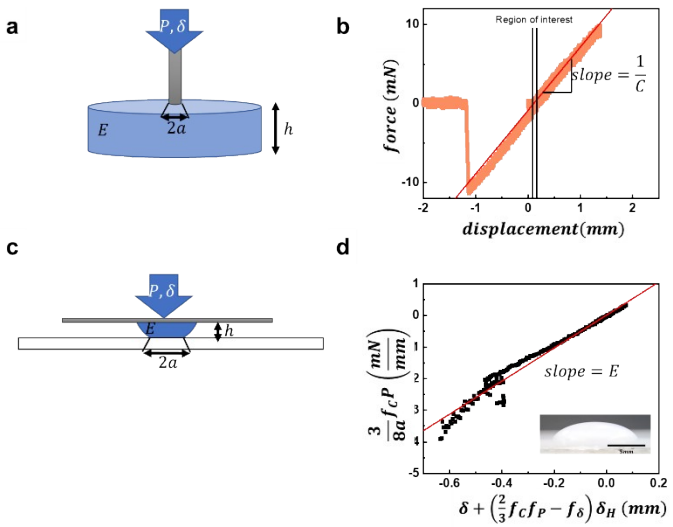


*Figure s1. Young's moduli measurement for PAM hydrogels. (a) The schematic of a flat probe indentation test on a soft substrate with thickness h. (b) The representative plot of a flat probe indentation test. The slope in the first 10% strain after contacting is for Young's modulus fitting. (c) The schematic of an indentation test to measure Young's modulus of the spherical hydrogel probe. (d) The linear fitting based on Equation s7. The slope is Young's modulus. Inset: side view photo of a PAM spherical probe.*

## S3 Finite element model for total strain energy in the void collapse inspection method

We use finite element modeling (FEM) to determine the prefactors of the total strain energy with respect to the separator thickness (t) and the normalized closed width ($^{w_c}/_{w}$). A 2-dimensional model of a solid circle with a rectangular void in the center is sketched. In the FEM, we determine the length with a unit of millimeter and the modulus with a unit of kilopascal. The ratio $^{w}/_{D} = \frac{15}{30} = 0.3$ is fixed based on the experimental geometries, and the thickness of the void (t) is varied. The constitutive relation is set as Neo-Hookean, Young's modulus is set as 1, and Poisson's ratio is set as 0.495 by altering the parameters of the model. We use the element type CPE4R for 2-dimentional plane strain modeling. When meshing the model, we assign 40 seeds to the width of the void and 50 seeds to the outer boundary of the circle by number. We assign the seeds to void thickness by size, with an interval distance ranging from 0.05 to 0.2, based on the void thickness. To simulate the strain energy in the deformed state, we set displacement boundary conditions at the width

edges of the rectangle. The region of the applied displacement boundary condition is centered with respect to the rectangular void. The displacement of either side is half of the void thickness, so the gap distance between the two widths is zero at the deformed state, which looks identical to the closed state. The outer surface of the model is pinned. The thicknesses of the void are 0.1, 0.2, 0.4, 0.8, 1.0, 1.5, 2.0, 2.4 and 3.0 for the strain energy versus thickness relationship. The rectangular void thicknesses are 0.8, 1.0, 1.5, 2.0 and 2.4 for the strain energy dependence of $f\left(\frac{w_c}{w}\right)$, during which the normalized closed width ranges from 0 to 1 with a step of 0.2. The total strain energy is collected from the history output function ALLSE.

Section 3.3.2 describes the closed width contribution $f$ as a 3-order polynomial function. The parameters {$m_1$, $m_2$, $m_3$, $m_4$} are {1.3948, -0.9290, 0.5337, 0.0011}, respectively. Noticing $m_4$ is the intercept, its zero value follows the requirement of $f(0) = 0$.

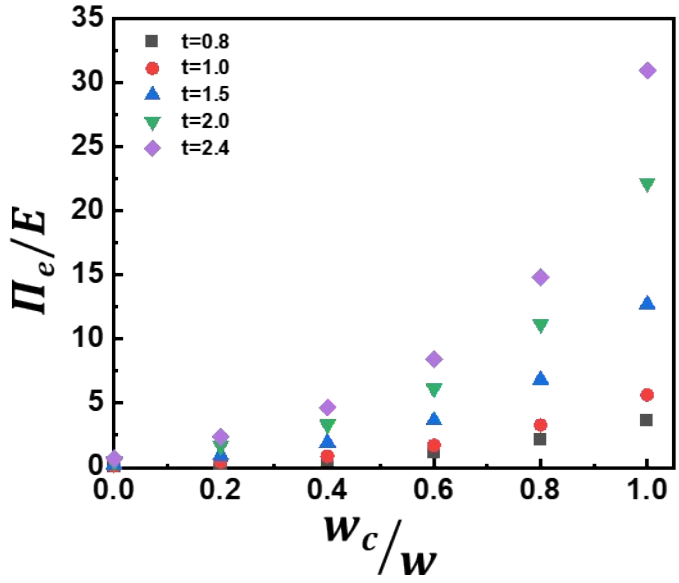


*Figure s2 FEA results of strain energy dependence of* $w_c/w$ *at different values of t. Figure 4(b) in the main text is developed from this data by normalizing the strain energy by the strain energy at the fully closed configuration,* $EKt^2$*, and plotting the normalized strain energy against* $w_c/w$*.*

## S4 Strain energy release rate of PAM-PAM contact

We measure the adhesion energy of the hydrogel interface by a force-based contact adhesion test on the Texture Analyzer. The spherical hydrogel probe is actuated to contact the hydrogel substrate (Figure s3(a)) at constant indenting and retracting speed of 0.01mm/s. The contact area is collected from the video taken by the camera, and the force, displacement, and time are collected from Texture Analyzer. The energy release rate, as a function of the contact radius, follows the following algorithm:

$$G = -\frac{(P' - P)^2}{4\pi a}\frac{dC}{da}. \quad \text{(s8)}$$

Here P is the force in the presence of adhesion energy, P' is the force in the absence of adhesion energy, and C is the compliance of the system[1,4].

In Equation s8, P' and C are theoretically derived. The compliance of the soft contact system (C) follows an additivity principle. The hydrogel probe and substrate share the same external force, so the system displacement consists of the displacement contributions from each segment of the series system, schematically shown in Figure s3(b). The displacement and the compliance can be modified with a correction factor of finite height separately, and the sum of the two compliances becomes the system compliance.

The system compliance is calculated as the following equation

$$C = C_{H,1} f_{C,1} + C_{H,2} f_{C,2}. \tag{s9}$$

where $C_{H,i} = \frac{1-\nu^2}{2E_i a}$ and $f_{C,i} = \left(1 + \frac{4}{3}\left(\frac{a}{h_i}\right) + \frac{4}{3}\left(\frac{a}{h_i}\right)^3\right)^{-1}$. Here $E_i$ is the $i^{th}$ Young's modulus of the hydrogel probe ($i = 1$) or the hydrogel substrate ($i = 2$), ν is Poisson's ratio, and $h_i$ is the thickness at the undeformed state of the hydrogel probe ($i = 1$) or the hydrogel substrate ( $i = 2$).

The force in the absence of adhesion energy is:

$$P' = \int_0^{\delta'} \frac{1}{C} d\delta = \int_0^{a} \frac{1 d\delta'}{C da'} da'. \tag{s10}$$

Here we choose the contact area as the independent variable, so we need to know the relationship between displacement in the absence of adhesion, denoted as δ' and a. The displacement in the absence of adhesion is

$$\delta_i' = \delta_H f_{\delta,i}. \tag{s11}$$

Here $\delta_H = \frac{a^2}{R}$ and $f_{\delta,i} = 0.4 + 0.6e^{-\frac{1.8a}{h_i}}$. The total displacement $\delta' = \delta_1' + \delta_2'$.

The soundness of Equation s10 is confirmed with finite element analysis. At the contact radius range that is observed in the experiment, ranging from 1.5mm to 2.5mm, the calculated P' is close to the reaction force simulated from FEA. We use an axisymmetric model in the FEM, and the geometrical features of the probe and substrate in the model are the same as the size in the experiment. The constitutive relationship is neo-Hookean, with $E_1$ and $E_2$ from previous tests and the same Poisson's ratio of 0.495. The bottom of the substrate is pinned, and the displacement is applied to the upper boundary of the probe. The force calculated from Equation s10 is close to the FEA result (Figure s3(c)).

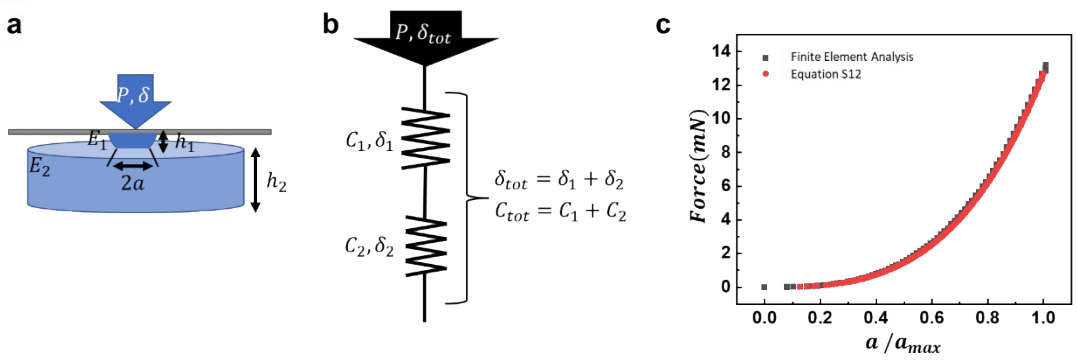


*Figure s3 The force in the absence of adhesion calculation. (a) The schematic of a force-based contact adhesion test. The hydrogel probe and substrate have individual moduli and thicknesses. (b) The schematic of the compliance additive principle. In a series system, the resistance force is constant regardless of the vertical location, and the displacement is additive. (c) The comparison of resultant forces between the FEA and the calculated result based on Equation s10. The contact radius range of Equation s10 is the same range as the contact radius in the experiment.*

## S4. Void collapse inspection method to calculate the $I_{EA}$ of PAM hydrogel interfaces

### S4.1 Derivation of $I_{EA}$ expression by $\left(\frac{w_c}{w}\right)_c$

The total energy density per unit length is the sum of strain energy and surface energy:

$$\frac{\Pi_{tot}}{E} = Kt^2 f\left(\frac{w_c}{w}\right) + l_{EA} w\left(1 - \left(\frac{w_c}{w}\right)\right). \quad \text{(s12)}$$

The partial derivative of Equation s12 to $\frac{w_c}{w}$ is:

$$\frac{d\left(\frac{\Pi_{tot}}{E}\right)}{d\left(\frac{w_c}{w}\right)} = Kt^2 f'\left(\frac{w_c}{w}\right) - l_{EA} w. \quad \text{(s13)}$$

Noticing that the second derivative $f''(x)$ is greater than zero in the interval $x \in [0,1]$, f' monotonically increases as $\frac{w_c}{w}$ increases in the interval. At this condition, the result of $\frac{d\left(\frac{\Pi_{tot}}{E}\right)}{d\left(\frac{w_c}{w}\right)} = 0$ indicates the minimum energy with respect to the closed width. By rearranging $\frac{d\left(\frac{\Pi_{tot}}{E}\right)}{d\left(\frac{w_c}{w}\right)} = 0$, the expression of $l_{EA}$ with respect to $\left(\frac{w_c}{w}\right)_c$ is derived, which is Equation 6 in the main text.

### S4.2 The closed width for partially closed configuration

We prepare four replicates hydrogel samples with the same components (5wt%, monomer: crosslinker =100:1) and the same separator thickness (0.79mm). The closed width $w_c/w$ is measured in the same vertical location for all four samples (Figure s4). We calculate the adhesion energy $G_c$ with $l_{EA}$ and Young's moduli of the hydrogels, as summarized in Table s1.

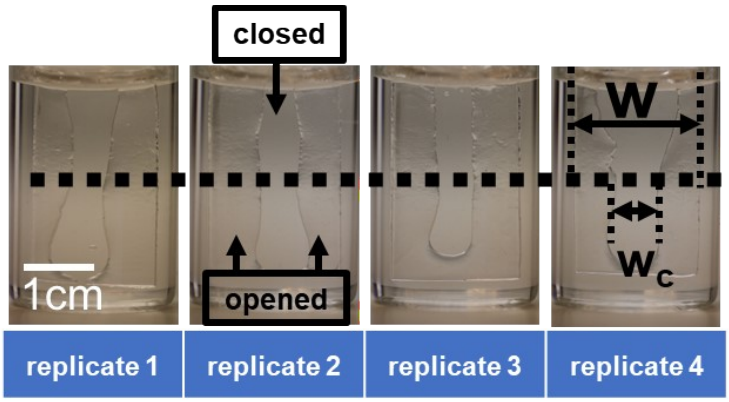


*Figure s4 The photos of hydrogel replicate to calculate the normalized closed width and the adhesion energy. We choose the steady state of the closed width after waiting for ~100 seconds. We choose the center region in the vertical direction to avoid the boundary conditions from the top and bottom. The closed center and opened edges are marked in replicate 2, and the total width and the closed width are marked in replicate 4.*

Table s1. Summary of four hydrogel replicates for the void collapse inspection method

| Replicate number | $t\ (mm)$ | $w_c/w$ | $t^2(mm^2)$ | $\frac{w}{Kf'\left(\frac{w_c}{w}\right)}(mm)$ | $l_{EA}(mm)$ |
|---|---|---|---|---|---|
| 1 | 7.94E-01 | 2.72E-01 | 6.30E-01 | 7.97E+00 | 7.91E-02 |
| 2 | 7.94E-01 | 2.85E-01 | 6.30E-01 | 7.82E+00 | 8.06E-02 |
| 3 | 7.94E-01 | 2.92E-01 | 6.30E-01 | 7.73E+00 | 8.15E-02 |
| 4 | 7.94E-01 | 3.32E-01 | 6.30E-01 | 7.10E+00 | 8.87E-02 |
| | | | Average | | 8.25E-02 |
| | | | Standard deviation | | 4.30E-03 |

## S5. Adhesion energy (critical energy release rate) in the force-based contact adhesion test

We regard the average value of the energy release rate in the interface separation region as the critical energy release rate, $G_c$. To find the critical value, we investigated the interfacial fracture behavior of the hydrogel by applying instant retractions and tracking the force relaxation. If the interface does not separate after the instant retraction for a certain duration (~100 seconds), the retraction is re-started to pull the probe back until the

interface is fully separated. In the tests, the instant retraction distance ($d_{re}$) is normalized by the indentation distance ($d_{ind}$).

The relative retraction distance $r = \frac{d_{re}}{d_{ind}}$ impacts the relaxation behavior of the hydrogel interface. When r is relatively small, the contact radius after instant retraction decreases and reaches a constant, and the energy release rate also goes to a constant value of approximately 0.25N/m. When the retraction starts, the energy release rate increases to another constant value of 0.35N/m. The width of the constant plateau decreases as the retraction distance increases, indicating that this critical value is related to the fracture of the hydrogel interface. When r increases further, the contact radius decreases spontaneously until the hydrogel interface fully separates, during which the calculated energy release rate reaches the plateau value related to the interface fracture (~0.35N/m). Based on the following observation, we conclude that the adhesion energy of the hydrogel interface, $G_c$ is the constant region of the energy release rate in the retraction process. The force, normalized displacement, normalized contact radius, and energy release rate are shown in Figure s5 for different instant retractions.

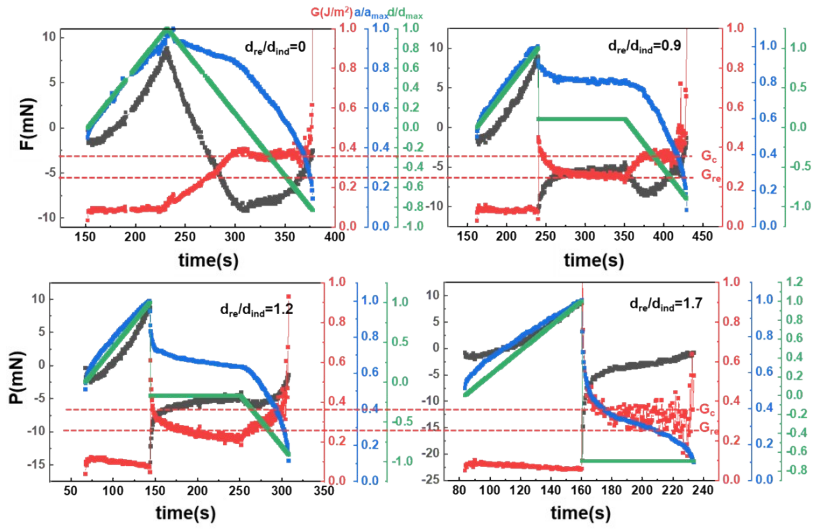


*Figure s5 Force-based contact adhesion tests with instant retractions. Synchronized plots of contact adhesion tests with a cylindrical substrate which is contacted with PTFE during curing. The retraction distances, normalized with the indentation distance, are marked in each plot.*

## S6. P-test of Adhesion energy (critical energy release rate) between the void collapse inspection method and force-based contact adhesion test.

We calculate the p-value based on two independent $l_{EA}$ values for the hypothesis test. For the $l_{EA}$ value from the void collapse inspection method, $\mu_1$=0.082, $s_1$=0.004, and $n_1$=4. For the $l_{EA}$ value of the force-based contact adhesion test, $\mu_2$=0.078, $s_1$=0.010, and $n_2$=4. We select four force-based contact adhesion tests, including one test in the main text and three tests in section S5 with different instant retractions, collect the critical energy release rate of the interface separating region, and calculate the $l_{EA}$ values by dividing them with $E_{avg}$. In the hypothesis test, the null hypothesis is "the difference between the two mean values equates to Δ, $\mu 1 - \mu 2 = \Delta$", while the alternative hypothesis is "the difference between the two mean values equates to Δ, $\mu 1 - \mu 2 \neq \Delta$" as a two-sided test. When Δ is equal to zero, the p-value is 0.491, which is much greater than the significance level of 0.05. The statistical analysis implies we don't have enough evidence to reject the null hypothesis at the significance level of 0.05. Thus, the two $l_{EA}$ values are consistent.

## References


1 A. J. Crosby and K. R. Shull, *J. Polym. Sci. Part B Polym. Phys.*, 1999, **37**, 3455–3472.

2 S. Rattan, L. Li, H. K. Lau, A. J. Crosby and K. L. Kiick, *Soft Matter*, 2018, **14**, 3478–3489.

3 K. L. Johnson, K. Kendall and A. D. Roberts, *Proc. R. Soc. A Math. Phys. Eng. Sci.*, 1971, **324**, 301–313.

4 K. R. Shull, *Mater. Sci. Eng. R Reports*, 2002, **36**, 1–45.

5 K. R. Shull, D. Ahn, W. L. Chen, C. M. Flanigan and A. J. Crosby, *Macromol. Chem. Phys.*, 1998, **199**, 489–511.